

Structure, ferromagnetic resonance, and permeability of nanogranular Fe-Co-B-Ni films

*Original*

Structure, ferromagnetic resonance, and permeability of nanogranular Fe-Co-B-Ni films / Pasquale, M; Celegato, F; Coisson, M; Magni, A; Perero, Sergio; Kabos, P; Teppati, Valeria; Han, S. H.; Kim, J; Lim, S. H.. - In: JOURNAL OF APPLIED PHYSICS. - ISSN 0021-8979. - 99:(2006). [10.1063/1.2165926]

*Availability:*

This version is available at: 11583/1801074 since:

*Publisher:*

AIP

*Published*

DOI:10.1063/1.2165926

*Terms of use:*

This article is made available under terms and conditions as specified in the corresponding bibliographic description in the repository

*Publisher copyright*

(Article begins on next page)

# Structure, ferromagnetic resonance, and permeability of nanogranular Fe–Co–B–Ni films

Massimo Pasquale,<sup>a)</sup> Federica Celegato, Marco Coisson, Alessandro Magni, and Sergio Perero

*Materials Department, IENGF, Strada delle Cacce 91, Torino IT 10135, Italy*

Pavel Kabos

*Electromagnetic Division, NIST, MS 104, 325 Broadway, Boulder, Colorado 80305-3328*

Valeria Teppati

*DELEN, Politecnico di Torino, Torino 24-10129, Italy*

Suk Hee Han

*Nano Device Research Center, KIST, Cheongryang, Seoul 130-650, South Korea*

Jongryoul Kim

*Department of Materials Science and Engineering, Hanyang University, Seoul 133-791, South Korea*

Sang Ho Lim

*Materials Science and Engineering, Korea University, Anam-dong Seongbuk-Gu, Seoul 136-701, South Korea*

(Presented on 2 November 2005; published online 20 April 2006)

The static and microwave magnetic properties of soft nanogranular  $(\text{Fe}_{0.7}\text{Co}_{0.3})_{71}\text{B}_{22}\text{Ni}$  films with a 2 T saturation magnetization are presented as functions of thickness, ranging from 136 to 235 nm. Microwave permeability values from 60 to 260 are measured and ferromagnetic resonance frequencies up to 6.8 GHz are found using a vector network analyzer, connected to coplanar/microstrip structures loaded with the ferromagnetic films. Topographic and magnetic structures down to 20–40 nm were observed by atomic/magnetic force microscopy. The combination of reasonable values of the permeability and high ferromagnetic resonance frequency makes these nanogranular materials useful in the development of inductive microwave components. © 2006 American Institute of Physics. [DOI: [10.1063/1.2165926](https://doi.org/10.1063/1.2165926)]

## I. INTRODUCTION

In recent years there has been a growing interest in the development of inductive elements based on conductive ferromagnetic materials for operation in the microwave region. This interest derives from tighter requirements on power saving, size reduction, and higher-frequency operation of microwave circuits intended for portable communication devices. Recently, Fe–Co-based thin films with a nanogranular structure have been shown to satisfy the above requirements. Improved microwave properties are obtained with a combination of high saturation induction and soft magnetic features.<sup>1–4</sup> This paper addresses the characterization and analysis of the static and microwave magnetic properties of  $(\text{Fe}_{0.7}\text{Co}_{0.3})_{71}\text{B}_{22}\text{Ni}_{7}$  nanogranular ferromagnetic films with a saturation magnetization  $M_S \approx 2$  T and a resistivity  $\rho \approx (8-9) \times 10^{-7} \Omega \text{ m}$ . The dc and high-frequency characteristics are presented as functions of thickness ranging from 136 to 235 nm. Permeability and ferromagnetic resonance (FMR) are measured up to 20 GHz with a vector network analyzer (VNA) connected to coplanar/microstrip structures loaded with ferromagnetic films.<sup>5,6</sup>

## II. EXPERIMENT

$(\text{Fe}_{0.7}\text{Co}_{0.3})_{71}\text{B}_{22}\text{Ni}_{7}$  nanogranular films with thickness  $t = 136-236$  nm were prepared on 200- $\mu\text{m}$ -thick Si substrates. An Fe–Co target with additional Ni and B chips was used for deposition by radio-frequency magnetron sputtering in an Ar atmosphere. The different thicknesses were obtained by varying the deposition time and were measured with a Tencor P10 profilometer. During the film preparation the background vacuum was maintained at a pressure less than  $9.3 \times 10^{-5}$  Pa. In order to induce an in-plane uniaxial magnetic anisotropy, the films were deposited in a static magnetic field of 80 kA/m produced by two permanent magnets positioned at the sides of the substrate. The films were finally cut into square samples ( $4 \text{ mm} \times 4 \text{ mm} \times 200 \mu\text{m}$ ) for further analysis.

The domain structures and topographies of the films were measured with an atomic/magnetic force microscope (AFM/MFM) with a spatial resolution better than 20 nm.<sup>7</sup> The AFM/MFM used for the imaging was a Digital Instruments multimode NanoScope scanning probe microscope operated in tapping and lift modes, with lift height ranging between 10 and 20 nm. The MFM tips (Veeco MESP-LC) used are coated with a soft Fe film of 50 nm nominal thickness and coercivity less than 80 A/m. The electrical resistivity  $\rho$  was measured using the four-probe method, along the direction transverse to the induced anisotropy. Magnetic

<sup>a)</sup>Electronic mail: [pasquale@ien.it](mailto:pasquale@ien.it)

TABLE I. Summary of the sample data: sample thickness  $t$ ; saturation magnetization  $M_s$ ; anisotropy field  $H_k$  derived from in-plane hard-axis AGFM measurements; in-plane easy-axis coercivity  $H_{c\text{-easy}}$ ; in-plane hard-axis coercivity  $H_{c\text{-hard}}$ ; dc permeability  $\mu_{dc}$  computed from  $M_s/\mu_0 H_k$ ; real part of the high-frequency permeability  $\mu'_{rf}$  measured with an impedance meter ( $L_R$ - $R_S$  measurement); ferromagnetic resonance (FMR) derived from  $S_{12}$  measurements; and resistivity  $\rho$  (four-point measurement).

Sample	$t$ (nm)	$M_s$ (T)	$H_k$ (A/m)	$H_{c\text{-easy}}$ (A/m)	$H_{c\text{-hard}}$ (A/m)	$\mu_{dc}=M_s/H_k$	$\mu'_{rf}(L_R)$	FMR (GHz)	$\rho$ ( $10^{-7} \Omega \text{ m}$ )
OAN5-4	136	2.12	28 000	96	920	60	57	6.81	8.43
OAN4-6	180	2.08	7840	96	400	212	201	4.2	8.1
OAN6-6	195	2.05	8320	112	504	197	191	3.95	9.26
OAN3-6	236	2.06	5920	40	168	278	264	3.8	8.97

properties were measured with different techniques. A Princeton MicroMag 2900 alternating-gradient field magnetometer (AGFM) was used to measure the out-of-plane and in-plane hysteresis loops, along the easy and hard axes. Surface magnetic properties were characterized using a longitudinal magneto-optical Kerr-effect setup (MOKE). The MOKE measurements were performed in the film plane using a polarized He-Ne laser light source with a  $1 \text{ mm}^2$  spot size. The complex permeability was measured performing a differential  $L_R$ - $R_S$  measurement from 40 Hz to 110 MHz, in the presence and absence of the films, using an impedance analyzer (Agilent 4294A) and a 10-mm-long nine turns solenoid. At higher frequencies ( $f < 8 \text{ GHz}$ ) the permeability was extracted from two-port VNA (Anritsu 37397C, 40 MHz–65 GHz) measurements of the  $S$  parameters<sup>5,6</sup> using a microstrip/coplanar line deposited on an alumina substrate. The films were positioned face down on a 20- $\mu\text{m}$ -thick dielectric foil covering the microstrip, with the easy axis oriented along the line. The microstrip was connected to the VNA using a universal test fixture (Anritsu 3680V). The ferromagnetic resonance frequency was tuned by varying the applied dc field (in-plane easy axis) from 0 to 8 kA/m with a pair of Helmholtz coils.

### III. RESULTS AND DISCUSSION

Four different  $(\text{Fe}_{0.7}\text{Co}_{0.3})_{71}\text{B}_{22}\text{Ni}_7$  film samples were characterized as a function of thickness with the techniques described in the previous section. The results are summarized in Table I.

AGFM measurements, performed in-plane along the easy axis, show coercivities as low as  $H_c = 50 \text{ A/m}$ . The magnetization curves of Figs. 1 show that a definite magnetic softening occurs in both the easy and hard in-plane directions with increasing thickness. The softening is particularly important along the hard axis, and the values of  $H_{c\text{-hard}}$  become comparable to the easy-axis values  $H_{c\text{-easy}}$  [see the data summary in Figs. 2(a) and 2(b)]. The analyses of in-plane magnetization curves lead to estimates of the anisotropy fields of the order of  $H_k \approx 6\text{--}8 \text{ kA/m}$ , indicating that the strong magnetocrystalline anisotropy associated with Fe-Co is partly suppressed by the magnetic domain structure encompassing several nanograins.<sup>8</sup> The anisotropy field suppression is significantly smaller in the case of the 136 nm film, where a much higher value of  $H_k \approx 28 \text{ kA/m}$  is observed, a result already obtained in other nanostructured Fe-Co films.<sup>9</sup> The high saturation magnetization values  $M_s \sim 2.0\text{--}2.1 \text{ T}$  are di-

rectly connected to the high Co content, which hinders the  $M_s$  decrease associated with the addition of B and Ni. The in-plane AGFM curves are confirmed by surface MOKE measurements, within the uncertainties due to the different technique and observation area.

The analysis of topographic tapping-mode AFM measurements show that the average grain size is close to 40 nm for all the films analyzed, independent of film thickness. The MFM images measured with a soft Fe tip (Fig. 1) reveal a well-defined in-plane domain nanostructure consisting of small chains of nanograins elongated in the easy-axis direction and also a small out-of-plane magnetization component compatible with the observed out-of-plane hysteresis loops [Fig. 1]. The magnetic domains and the underlying nanogranular structure, observed on the 136-nm-thick film, are shown in Fig. 1. The dark/light stripes indicate the presence

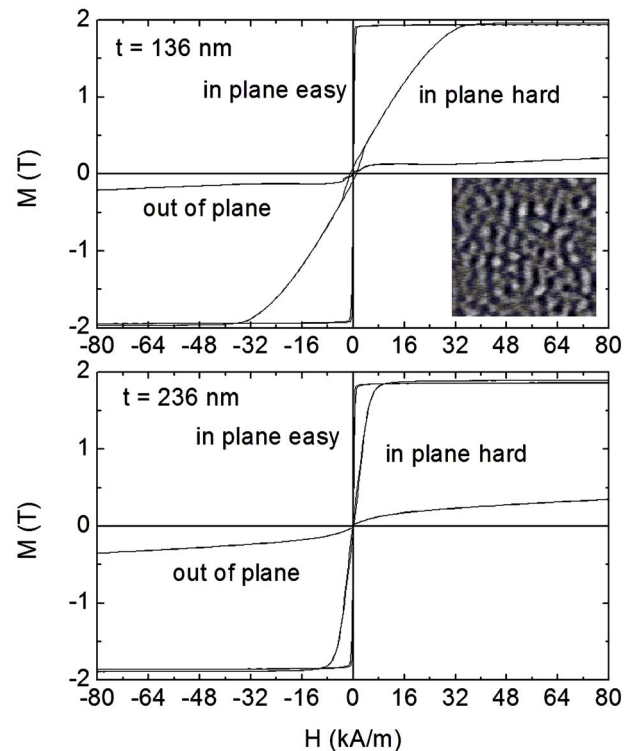


FIG. 1. Magnetization curves measured by AGFM in-plane and out-of-plane on the thinnest and thickest Fe-Co-B-Ni thin films. Inset: MFM lift mode image (frequency) showing a nanogranular magnetic structure. Scan size  $500 \times 500 \text{ nm}$ . The lighter/darker regions, elongated in the induced anisotropy (up-down) direction, are connected magnetization components magnetic domains.

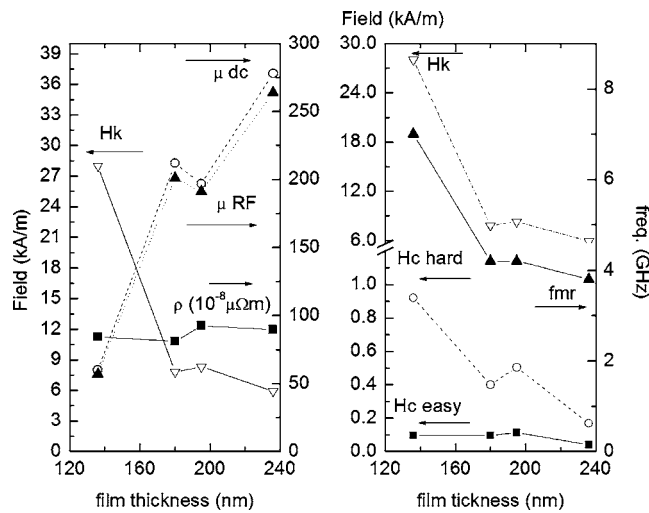


FIG. 2. (a) (Left): Anisotropy field  $H_K$  (open triangles, left y axis); dc permeability derived from Fig. 1 (open dots, right y axis); resistivity (black squares, right y axis); and rf permeability (black triangles, right y axis). (b) (Right): Anisotropy field  $H_K$  (open triangles, left y axis); hard axis in-plane coercivity (open dots, left y axis); easy-axis in-plane coercivity (black squares, left y axis); and ferromagnetic resonance frequency (black triangles, right y axis).

of an in-plane component of the magnetization associated with a domain. The domains are spatially correlated to the grain topography: each dark/light region typically encompasses a few nanograins aligned in the induced anisotropy direction. Equivalent domain structures were found in all the films, a result associated with the similar AGFM magnetic behavior. The measured resistivity values range between  $\rho = 8 \times 10^{-7}$  and  $9.3 \times 10^{-7} \Omega \text{ m}$  due to an incomplete electrical isolation of the nanograins.<sup>7</sup> It is particularly interesting to note that there is at least a partial correspondence between the fluctuations observed in the resistivity and the anisotropy field  $H_K$ , as determined from hard-axis in-plane magnetization curves [Fig. 2(a)]. This effect is related to the superposition between the nanostructure and the domain structure, and it is an additional evidence of the close relation between the topology of the metallic nanograins and the magnetic properties.<sup>9</sup>

The variations of the low-field FMR frequency (Fig. 3), which is proportional to  $\sqrt{(M_s H_K)}$ , closely match the changes of the anisotropy field  $H_K$  with thickness, as shown in Fig. 2(b). A maximum FMR frequency of 6.8 GHz is found in the case of the 136-nm-thick film, which possesses a particularly high value of anisotropy. As expected, the FMR frequency shifts to higher values when a dc magnetic field up to 8 kA/m is applied in the field plane along the easy direction. The observed field dependence of the frequency shift corresponds to Kittel's formula for the thin-film geometry.<sup>10</sup>

The relative permeability, determined from the static

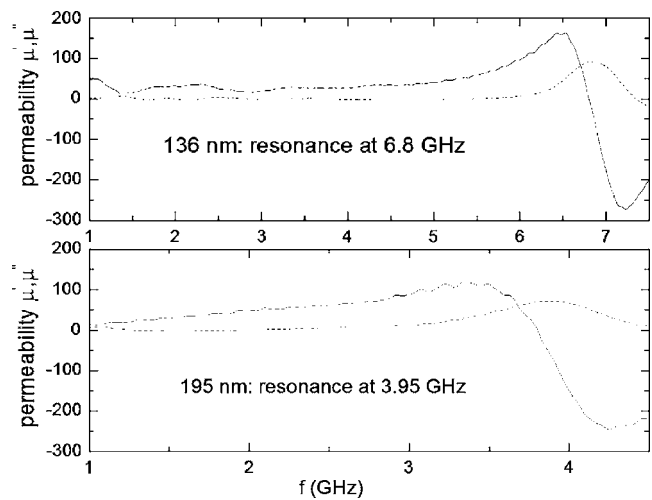


FIG. 3. Complex permeability ( $\mu'$  continuous lines and  $\mu''$  dashed lines) of two Fe-Co-B-Ni nanogranular films of different thicknesses. Top: 136-nm-thick film with a 6.8 GHz ferromagnetic resonance; bottom: 197-nm-thick film with a resonance of 3.95 GHz.

AGFM magnetization curves, shows values between  $\mu_r \approx 60$  and 278, while MHz-range inductance measurements made with an impedance meter lead to slightly lower values of the real part of the permeability  $\mu'_r$  between 57 and 264 (see Table I and Fig. 3). The particular combination of the measured values of permeability and high FMR frequency show promise for the use of these nanogranular materials in the development of microwave circuit components in a band up to 5–6 GHz.

## ACKNOWLEDGMENTS

This work was partly supported by the Italy-Korea bilateral scientific cooperation program “*Nanogranular magnetic films and devices for GHz frequency applications*” funded by the Italian Ministry of Foreign Affairs and the Korean Ministry of Research.

- <sup>1</sup>S. Ohnuma, H. Fujimori, T. Masumoto, X. Y. Xiong, D. H. Ping, and K. Hono, Appl. Phys. Lett. **82**, 946 (2003).
- <sup>2</sup>M. Ohnuma, K. Hono, E. Abe, H. Onodera, S. Mitani, and H. Fujimori, J. Appl. Phys. **82**, 5646 (1997).
- <sup>3</sup>G. S. D. Beach and A. E. Berkowitz, IEEE Trans. Magn. **41**, 2043 (2005).
- <sup>4</sup>J. C. Sohn, D. J. Byun, and S. H. Lim, Phys. Status Solidi A **201**, 1786 (2004).
- <sup>5</sup>J. C. Sohn, D. J. Byun, S. H. Lim, S. H. Han, and M. Yamaguchi, Digests of the IEEE International Magnetism Conference 2005, 4–8 April 2005, Nagoya, Japan, pp. 1107–1108.
- <sup>6</sup>W. Barry, IEEE Trans. Microwave Theory Tech. **MTT-34**, 80 (1986).
- <sup>7</sup>Y. Martin and H. K. Wickramasinghe, Appl. Phys. Lett. **50**, 1455 (1987).
- <sup>8</sup>J. C. Sohn, D. J. Byun, and S. H. Lim, J. Magn. Magn. Mater. **272–276**, 1500 (2004).
- <sup>9</sup>M. Pasquale, C. P. Sasso, F. Celegato, J. C. Sohn, and S. H. Lim, J. Appl. Phys. **97**, 10N306 (2005).
- <sup>10</sup>C. Kittel, Phys. Rev. **73**, 155 (1948).